

DUAL-POLARIZATION, MOBILE, X-BAND, DOPPLER-RADAR OBSERVATIONS  
OF HOOK ECHOES IN SUPERCELLS

Francesc Junyent Lopez<sup>1</sup>, A. Pazmany<sup>1</sup>, H. Bluestein<sup>2</sup>, M. R. Kramar<sup>2</sup>, M. French<sup>2</sup>, C. Weiss<sup>2</sup> and S. Frasier<sup>1</sup>

<sup>1</sup> University of Massachusetts, Amherst, Massachusetts

<sup>2</sup> University of Oklahoma, Norman, Oklahoma

### 1. ABSTRACT

Since 1993, the University of Massachusetts Microwave Remote Sensing Laboratory and University of Oklahoma School of Meteorology have collaborated in the study of severe storms and tornadoes conducting field experiments with mobile radars (Bluestein and Pazmany, 2000). One of the radar systems is a 9.4 GHz polarimetric Doppler radar, developed to provide storm-scale observations complementing existing very high resolution, but limited range, W-band observations. In addition to providing real-time surveillance of reflectivity, the X-band radar can record time series data from which co-polarized reflectivity for H and V polarization ( $Z_{HH}$  and  $Z_{VV}$ ), differential reflectivity ( $Z_{DR}$ ), specific differential phase shift (Kdp), cross-correlation coefficient ( $\rho_{HV}$ ), and Doppler velocity are estimated to 30 km in range.

This paper documents close range, high resolution reflectivity, Doppler velocity, differential reflectivity, and cross-correlation observations of hook echoes in tornadic supercells obtained on 12 May 2004. A variety of fine scale features are observed, including a clear tornado signature in the polarimetric fields. Power-weighted Doppler distributions, analogous to Doppler spectra, are obtained in the vortex area.

### 2. INTRODUCTION

The need for accurate warning and detection of severe weather, together with scientific research dedicated to understand and characterize its nature, has driven radar tornado probing and detection as an important research topic that has added significantly to the understanding of such severe weather phenomena.

There has been a progression in the techniques and equipment used for that purpose: Initially, the detection of a tornado relied on the storm hook echo reflectivity signature, and the addition of Doppler information allowed the correlation of the hook echo with an associated strong circulation radial velocity couplet. However this is not conclusive evidence of a tornado, nor does it guarantee accurate detection of all of them. The relative size of the tornado and radar antenna beam smoothes

out its signature (Brown, 1998), and the radar beam elevation and range set the minimum height at which this can be obtained. This resolution and elevation problem can be overcome with the use of mobile radars, while increasing the number of cases.

Recently, two new approaches to the tornado detection problem have been developed. The use of S-Band polarimetric radar has shown evidence of combined  $Z_{DR}$  and  $\rho_{HV}$  signatures in the debris field (Ryzhkov, 2003), and the use of Doppler spectrum for tornado detection has been investigated (Yu et al., 2003), showing potential for detection even when the tornado is fully encompassed by the radar beam. This new approaches can also benefit from mobile radar implementation, helping detect and characterize smaller and weaker tornadoes that go more easily undetected by the larger fixed systems.

### 3. MOBILE RADAR DESCRIPTION

The UMass XPol radar (Pazmany et al., 2003) is a truck mounted pulse Doppler radar with a 1.8 m dual polarized antenna, mounted on an elevation-over-azimuth pedestal. The radar uses a magnetron to generate high-power microwave pulses, and two parallel receivers simultaneously amplify and down-convert incoming target echoes at horizontal and vertical polarization. The conventional coherent-on-receive technique is used for pulse pair Doppler velocity measurements, and a staggered pulse repetition frequency allows to increase the maximum unambiguous velocity while maintaining an adequate unambiguous range (Zrnich and Mahapatra, 1985).

The radar operator can select between two modes of operation: *Surveillance* mode displays long-range, low data-rate averaged reflectivity data and *Raw* mode records IF-offsetted time series data to compute co-pol reflectivity at H and V polarization ( $Z_H$  and  $Z_V$ ), differential reflectivity ( $Z_{DR}$ ), specific differential phase ( $K_{DP}$ ), cross-correlation coefficient ( $\rho_{HV}$ ) and Doppler velocity mean and standard deviation (Doviak and Zrnich, 1984; Bringi and Chandrasekar, 2001). Table 1 lists the significant radar parameters.

### 4. DATA COLLECTION AND PROCESSING

During the 2004 spring tornado season XPol was deployed in many tornadic and nontornadic supercells,

<sup>0</sup>Corresponding author adress: Francesc Junyent Lopez, Microwave Remote Sensing Laboratory., ECE, University of Massachusetts, Amherst; e-mail: [junyent@mirsl.ecs.umass.edu](mailto:junyent@mirsl.ecs.umass.edu)

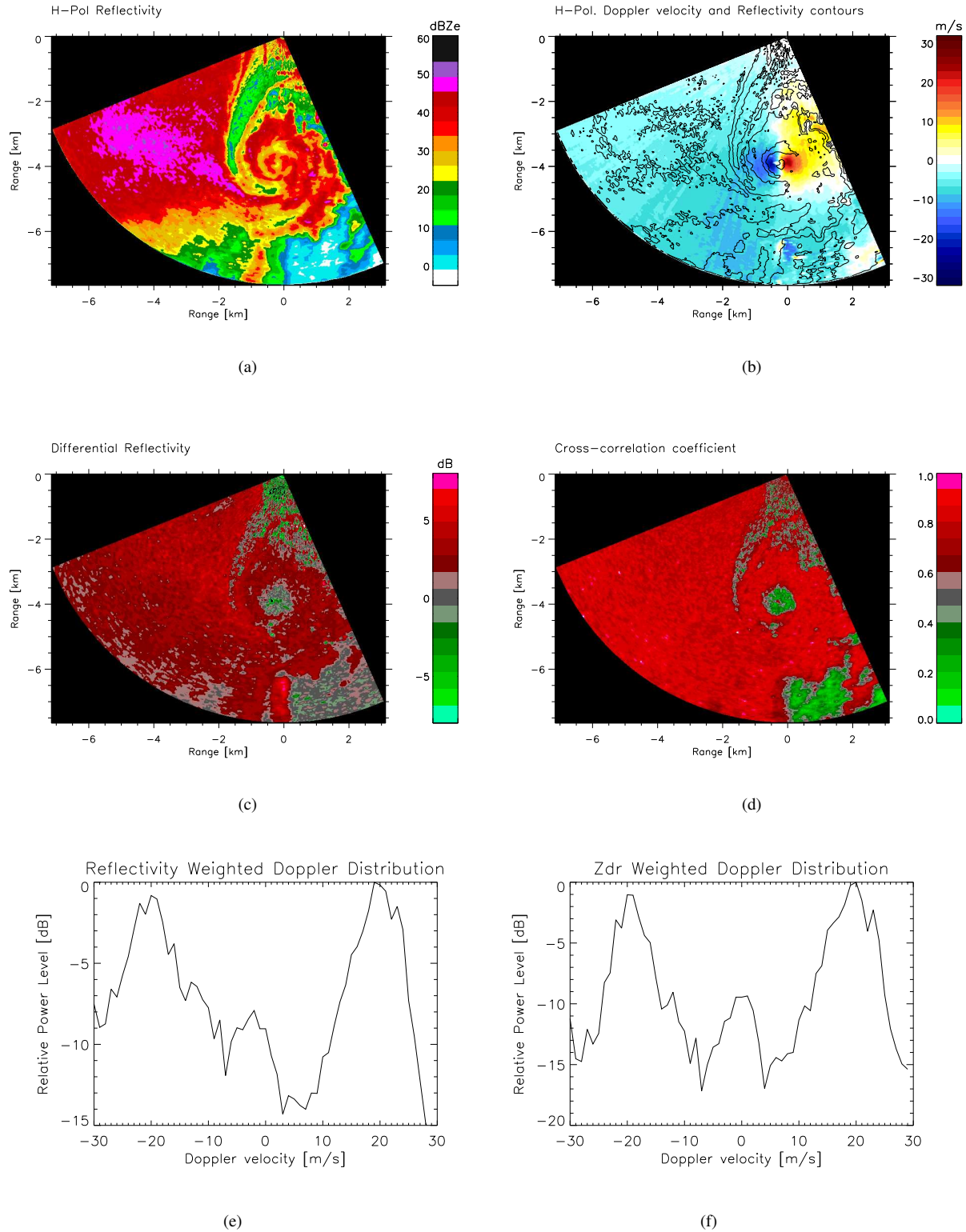


Fig. 1. Tornado radar images obtained near Attica, KS on 12 May 2004. Deployment coordinates were  $37^{\circ} 16.5' N$   $98^{\circ} 32.9' W$  and time was 7:55 PM CDT. XPol was operated in a 7.5 km range and  $3^{\circ}$  of elevation. (a) Horizontal polarization reflectivity (b) Horizontal polarization Doppler velocity, with superimposed 15 dB horizontal reflectivity contours (c) Differential reflectivity (d) Cross-correlation coefficient (e)(f) Reflectivity and Diff. reflectivity weighted Doppler distributions obtained in a  $750 \times 350 m^2$  ( $Az \times Range$ ) box enclosing the vortex.

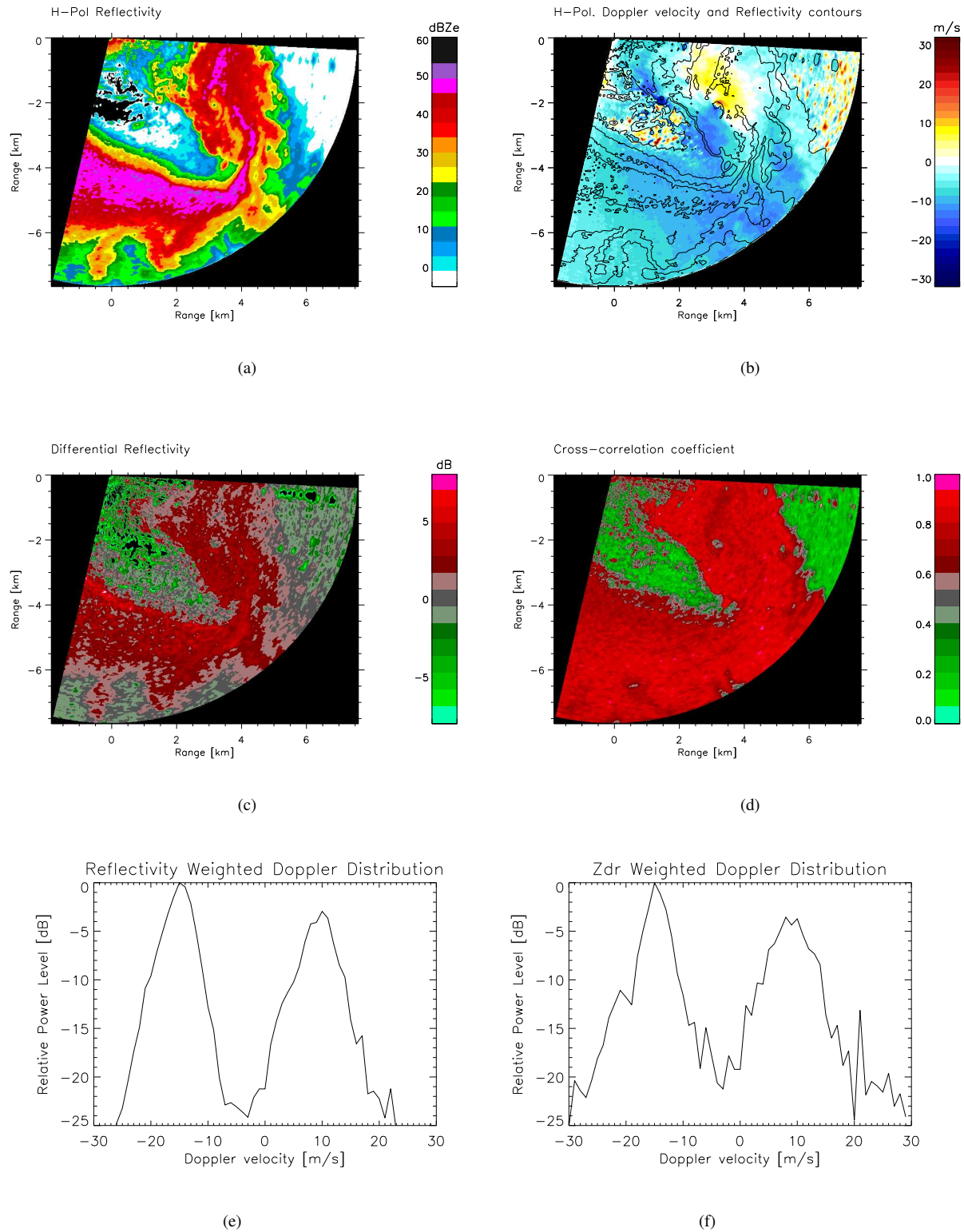


Fig. 2. Tornado radar images obtained between Attica and Harper, KS on 12 May 2004. Deployment coordinates were  $37^{\circ} 14.9' N$   $98^{\circ} 02.4' W$  and time was 8:25 PM CDT. XPol was operated in a 7.5 km range and  $3^{\circ}$  of elevation. (a) Horizontal polarization reflectivity (b) Horizontal polarization Doppler velocity, with superimposed 15 dB horizontal reflectivity contours (c) Differential reflectivity (d) Cross-correlation coefficient (e)(f) Reflectivity and Diff. reflectivity weighted Doppler distributions obtained in a  $750 \times 350 m^2$  ( $Az \times Range$ ) box enclosing the vortex.

TABLE I  
XPOL RADAR CHARACTERISTICS

<b>Transmitter</b>	
Center frequency	9.41 GHz
Peak power output	25 kW
Pulse width	1 $\mu$ s
Polarization	Equal power, simultaneous V & H
PRF	Staggered, 1.6 - 2.0 kHz
Max. Unambiguous velocity	$\pm 60$ m/s
Max. Unambiguous range	75 km
<b>Antenna and Pedestal</b>	
Type (size)	Dual-polarized parabolic reflector (1.8 m)
3-dB Beamwidth	1.25 $^\circ$
Gain	41 dB
Max. scan rate	24 $^\circ$ /s in Az and El
<b>Receiver</b>	
Dynamic Range	70 dB
Noise figure	4 dB
Bandwidth	4.5 MHz
First IF	62.5 MHz
Second IF	2.5 MHz
Min. detectable signal	-5 dBz @ 10 km

adding to the already extensive 2001, 2002 and 2003 data set. On 12 May 2004 two data sets were obtained in which two tornadoes were probed at very close range (less than 5 km from the radar, corresponding to an azimuthal resolution better than 150 m). The proximity to the radar increases the azimuthal resolution and signal-to-noise ratio of the obtained measurement, which allows the depiction of weaker, finer scale structures and decreases the measurement final standard deviation.

Figure 1 shows F2 level tornado radar images obtained in a deployment near Attica, KS (Lat: 37 $^\circ$  16.5' N, Lon: 98 $^\circ$  32.9' W) on 12 May 2004 at 7:55 PM CDT. The horizontal polarization reflectivity image (a) shows a well defined toroid structure corresponding to the funnel cloud, with weaker reflectivity in the center. The funnel is surrounded by swirls of what probably is centrifuged dust and rain, and located at the tip of a highly reflective hook echo. A clear notch in reflectivity appears between the tornado and the parent storm. The Doppler image (b) shows very symmetric velocity couplets around the vortex, peaking at around  $\pm 22$  m/s. High spatial correlation is observed between the center of the vortex Doppler signature and the weaker reflectivity region corresponding to the inner funnel. The polarimetric images (c) and (d) show a very distinct tornado signature: In a 1 km diameter disc centered at the tornado vortex, corresponding to the tornado debris field,  $Z_{DR}$  takes values around and close to zero dB, indicative of random scatterer orientation, and the cross-correlation coefficient is below 0.5, owing to the non-meteorological nature of the scatterers. In the swirls

surrounding the tornado debris signature both  $Z_{DR}$  and cross-correlation coefficient increase, achieving values usually associated with the presence of hydrometeors ( $Z_{DR}$  ranges from 1.5 to 4 dB,  $\rho_{HV}$  is greater than 0.8). This new X-Band observation is consistent with previous ones at S-Band (Ryzhkov, 2003) and adds to the potential of polarimetric tornado detection.

Figure 2 shows data from another 12 May 2004 tornado that touched down southwest of Harper, KS. The radar was deployed at 8:25 PM at coordinates 37 $^\circ$  14.9' N 98 $^\circ$  02.4' W. The tornado vortex is again at the tip of a very reflective hook echo, embedded in a low-level mesocyclone. The vortex shows a small eye, with a diameter of about 150 m, with a clear reflectivity drop. In (c) and (d), in the same eye region, the tornado polarimetric signature previously described is observed again. The smaller size of it, related to the tornado debris field, is commensurate with the tornado F0 damage level.

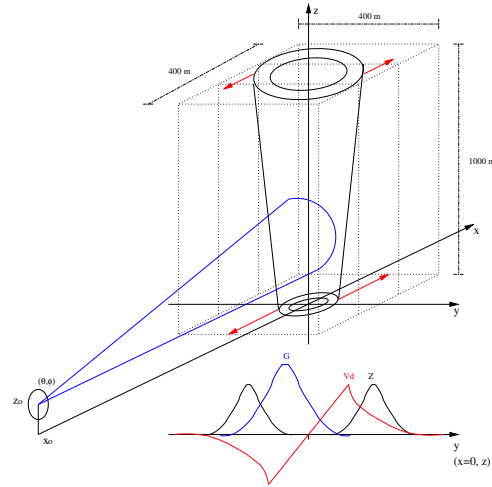


Fig. 3. Vortex radar spectrum simulation

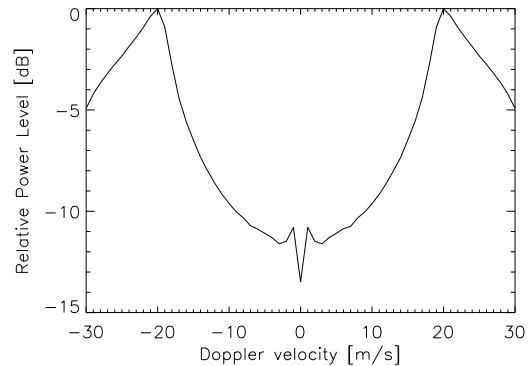


Fig. 4. Simulated Doppler spectra

Images (e) and (f) in both Figure 1 and Figure 2 show power-weighted histograms of Doppler velocity calculated in a  $750 \times 350 \text{ m}^2$  ( $Az \times \text{Range}$ ) box enclosing the vortex. These distributions are only approximations of the true Doppler spectra, which for the XPol radar cannot be easily obtained in the frequency domain due to the combination of the staggered PRF scheme employed plus the additional inter-pulse period needed to maintain the magnetron duty cycle. These distributions are obtained as power-Doppler velocity histograms with non-averaged samples, and match qualitatively the expected shape of the Doppler spectra (Bluestein et al., 1993; Doviak and Zrnice, 1984). A simulation is performed in which the radial component of a cylindrically symmetric Rankine vortex velocity field is combined with Gaussian distributions of reflectivity corresponding to the funnel walls. The ensemble has conic shape along the  $z$  axis and has angular momentum conservation in the velocity field. The simulation domain is divided in three regions, corresponding to three radar resolution volumes, and probed by a pencil beam antenna. Figure 3 illustrates the simulation scheme.

Adjusting the simulation parameters to the conditions in which Figure 1 data was obtained results in the Doppler spectra shown in Figure 4 (obtained as the addition of powers at 1 m/s velocity bins, corresponding to the center resolution volume of the simulation probed by a non-scanning antenna), whose shape agrees with that of Figure 1 (e) and (f).

## 5. SUMMARY

In this paper we have presented X-Band mobile radar, high-resolution tornado data showing evidence of a polarimetric signature in the tornado debris field proportional to the tornado damage level. Also, power-weighted Doppler distributions are obtained in the vortex area, and found to be in agreement with tornado spectrum measurements available in the literature and a simple 3-D model of a tornado used to obtain ideal Doppler spectra.

## 6. ACKNOWLEDGMENTS

This work was funded by NSF grants ATM-9616730 at UMass and ATM-0241037 at OU, and sponsored in part by the Engineering Research Centers program of the National Science Foundation under NSF Award #0303747. We also acknowledge Mark Laufensweiler, Brad Barrett, Dan Dawson, Kery Hardwick and Chad Baldi for all their help.

## 7. REFERENCES

Bluestein, H. B. and A. L. Pazmany, 2000: Observations of tornadoes, and other convective phenomena with a mobile, 3-mm wavelength, Doppler radar: The Spring 1999 field experiment, *Bull. Amer. Meteor. Soc.*, **70**, 1514-1525.

Bluestein H.B., Ladue J. G., Stein H. and Spehger D. and W. P. Unruh, 1993: Doppler radar wind spectra of supercell tornadoes, *Monthly Weather Review*, **121**, 2200-2221.

Brown, A. R., 1998: Nomogram for aiding the interpretation of tornadic vortex signatures measured by Doppler radar, *Wea. Forecasting*, **13**, 505-512.

Brangi, V.N and V. Chandrasekar, 2001: *Polarimetric Doppler weather radar*, Cambridge, University Press.

Doviak, R. J. and D.S. Zrnice, 1984: *Doppler radar and weather observations*, New York, Academic Press.

Pazmany, A. L., Junyent Lopez, F., Bluestein, H. B. and M. Krammar, 2003: Quantitative Rain Measurements with a Mobile, X-Band, Polarimetric Doppler Radar, *31st Int. Conf. on Radar Meteor.*, **P5B.3**.

Ryzhkov, A., 2003: Polarimetric tornado detection, *NSSL Briefings*, [www.nssl.noaa.gov/briefings/vol5no3/polarimetric.html](http://www.nssl.noaa.gov/briefings/vol5no3/polarimetric.html).

Yu, T., Zrnice, D., Shapiro A. and M. B. Yeary, 2003: Feasibility of earlier tornado detection using Doppler spectra, *31st Int. Conf. on Radar Meteor.*, **5A.7**.

Zrnice D.S. and P. Mahapatra, 1985: Two methods of ambiguity resolution in pulse Doppler weather radars, *IEEE Trans. on Aero. and El. Syst.*, **4**, 470-483.